

# The net carbon flux due to deforestation and forest re-growth in the Brazilian Amazon: analysis using a process-based model

ADAM I. HIRSCH\*, WILLIAM S. LITTLE†, RICHARD A. HOUGHTON\*, NEAL A. SCOTT\* and JOSEPH D. WHITE‡

\*The Woods Hole Research Center, PO Box 296, Woods Hole, MA 02543, USA, †The Woods Hole Oceanographic Institution, Woods Hole, MA 02543, USA, ‡Baylor University, PO Box 97388, Waco, TX 76798, USA

## Abstract

We developed a process-based model of forest growth, carbon cycling and land-cover dynamics named CARLUC (for CARbon and Land-Use Change) to estimate the size of terrestrial carbon pools in terra firme (nonflooded) forests across the Brazilian Legal Amazon and the net flux of carbon resulting from forest disturbance and forest recovery from disturbance. Our goal in building the model was to construct a relatively simple ecosystem model that would respond to soil and climatic heterogeneity that allows us to study the impact of Amazonian deforestation, selective logging and accidental fire on the global carbon cycle. This paper focuses on the net flux caused by deforestation and forest re-growth over the period from 1970 to 1998. We calculate that the net flux to the atmosphere during this period reached a maximum of  $\sim 0.35 \text{ PgC yr}^{-1}$  ( $1 \text{ PgC} = 1 \times 10^{15} \text{ gC}$ ) in 1990, with a cumulative release of  $\sim 7 \text{ PgC}$  from 1970 to 1998. The net flux is higher than predicted by an earlier study (Houghton *et al.*, 2000) by a total of  $1 \text{ PgC}$  over the period 1989–1998 mainly because CARLUC predicts relatively high mature forest carbon storage compared with the datasets used in the earlier study. Incorporating the dynamics of litter and soil carbon pools into the model increases the cumulative net flux by  $\sim 1 \text{ PgC}$  from 1970 to 1998, while different assumptions about land-cover dynamics only caused small changes. The uncertainty of the net flux, calculated with a Monte-Carlo approach, is roughly 35% of the mean value (1 SD).

*Keywords:* Amazon basin, biosphere–atmosphere carbon flux, carbon cycle modeling, land-use change

*Received 1 November 2002; revised version received 24 July 2003 and accepted 29 August 2003*

## Introduction

There is an on-going effort to understand the impact of land-cover and land-use change on the global carbon cycle (Prentice *et al.*, 2001; Houghton, 2003), with particular focus on the Brazilian Legal Amazon (Houghton *et al.*, 2000; Potter *et al.*, 2001a) since this region contains half of Earth's remaining tropical rain forests and is experiencing rapid forest clearing. Deforestation in this region over the past three decades has affected  $10\,000\text{--}30\,000 \text{ km}^2 \text{ yr}^{-1}$ , causing a net

release of  $0.1\text{--}0.3 \text{ PgC yr}^{-1}$  (Houghton *et al.*, 2000), an amount that is significant in the global carbon budget and comparable with the interannual variability in net carbon exchange between the atmosphere and undisturbed forests due to climatic variability (Tian *et al.*, 1998; Asner *et al.*, 2000; Potter *et al.*, 2001b). At the same time, it is becoming clear that the area impacted by selective logging and accidental fire in the Amazon each year is of the same order of magnitude as annual deforestation (Nepstad *et al.*, 1999), causing a transfer of carbon to the atmosphere of uncertain magnitude. We developed a new numerical carbon cycle model, called CARLUC (for CARbon and Land-Use Change) that provides a framework to study the impacts of deforestation, selective logging, accidental fire and subsequent forest recovery on the global carbon budget. Here, we present results for the case of deforestation and forest re-growth in the Brazilian Legal Amazon.

Correspondence: Adam Hirsch, Cooperative Institute for Research in the Environmental Sciences, University of Colorado at Boulder, USA and Climate Monitoring and Diagnostics Laboratory, National Oceanic and Atmospheric Administration, 325 Broadway, Boulder, CO 80303-3328, USA, tel. +1 303 497 69999, fax +1 303 497 5590, e-mail: adam.hirsch@noaa.gov

A recent study (Houghton *et al.*, 2000) calculated a range of values of the net carbon flux due to land-use change in the Amazon from 1960 to 1998 using a carbon 'bookkeeping' model, annual rates of deforestation, and spatially detailed maps of deforestation, forest re-growth and forest biomass. Here, we examine three potential sources of uncertainty in the Houghton *et al.* (2000) study. First, we use a new, spatially explicit, process-based carbon cycle model (CARLUC) to predict mature forest carbon storage and forest re-growth rather than using digital biomass maps derived from forest inventory data and assuming that re-growth rate is proportional to mature forest biomass. Second, we use CARLUC to examine the contribution of litter and soil carbon to the net carbon flux associated with deforestation and re-growth. These carbon stocks were not included in the Houghton *et al.* (2000) study. Third, we examine different assumptions about how land-use dynamics affect the net carbon flux. Houghton *et al.* (2000) modeled agricultural abandonment as a fixed fraction of annual deforestation and assumed no re-clearing of secondary forest in order to match the proportion of deforested lands observed to be re-growing forest in a 1986 land-cover map derived from Landsat data. Here, we assume that land spends a characteristic time under agriculture before being abandoned, and then a characteristic time as secondary forest before being re-cleared for another round of agriculture. The turnover time of agricultural land and re-growing forest was derived by matching the time series of agricultural and secondary forest total area derived from a time series of land-cover classification maps made available by the Tropical Rainforest Information Center (TRFIC) at Michigan State University.

We verify CARLUC predictions of both mature forest carbon storage and carbon accumulation in re-growing forests with observations or simple models derived from empirical data. We also test the model's predictions for live aboveground biomass, coarse woody debris, fine litter fall and wood growth with independent observations. The sensitivity of mature forest carbon storage to different model parameters, and the uncertainty in our net flux and carbon storage values are also addressed.

**Methods**

*Overview of the CARLUC model*

CARLUC is composed of five submodels: (1) forest primary productivity, based on the 3-PG (physiological principles in predicting growth) model (Landsberg & Waring, 1997); (2) carbon allocation and turnover of live C pools in undisturbed forests, based on the approach

taken by NASA-CASA (Potter *et al.*, 1998); (3) decomposition of dead organic matter, based on the Roth-C model (Jenkinson, 1990); (4) transfers between different compartments of the carbon model due to forest disturbance, from the WHRC Carbon Bookkeeping Model (Houghton *et al.*, 2000); and (5) land-cover dynamics, which can either be taken from the literature (e.g. Houghton *et al.*, 2000) or inferred from a time series of satellite derived land-cover maps of the Brazilian Amazon, as described below.

In the model, carbon enters the forest through net primary production (Fig. 1). It is then allocated between wood, leaf and fine roots using fixed allocation parameters. Leaves and fine roots eventually die and enter fine detritus pools, while wood passes to a coarse detritus pool. Fine and coarse detritus decompose, returning some of the carbon to the atmosphere, while the remainder passes to soil humus, which also decomposes, but more slowly. Deforestation causes a redistribution of the ecosystem carbon pools, combusting wood and aboveground litter, creating inert charcoal and sending a large fraction of live wood to woody debris, which is either combusted, converted to charcoal, or left to decompose. A small fraction of wood is passed to a 'wood product' pool that decays over time.

The following sections will present the structure of each submodel including the parameter values chosen for the Amazon basin, the details of the net flux calculation, and the procedure used for sensitivity testing of CARLUC.

*Forest productivity modeling*

We based the **net primary productivity (NPP)** calculation on algorithms in the 3-PG model because it is a general model based on physiological principles that

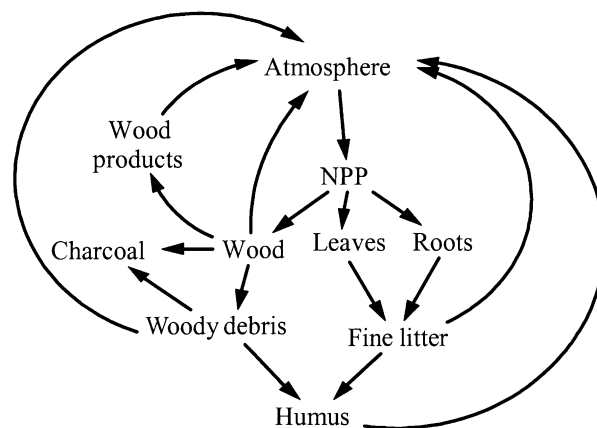


**Fig. 1** Diagram of carbon flows in the CARLUC (CARbon and land-use change) model.

should apply across different forest and biome types (Landsberg & Waring, 1997), yet captures the influence of climate and soil variability on forest growth. NPP is calculated monthly, to capture seasonality of climate in the Amazon, but in this paper interannual variability is not considered. The following equations are used for the NPP calculation:

$$\text{NPP} = c_{\text{pp}} \times \text{GPP}, \quad (1a)$$

$$\text{GPP} = 0.012 \times \alpha \times \text{uAPAR}, \quad (1b)$$

$$\text{uAPAR} = \text{APAR} \times \text{MIN}(f_{\theta}, f_D) f_T, \quad (1c)$$

$$\text{APAR} = \text{PAR}_0 \times (1 - e^{-\lambda \times \text{LAI}}). \quad (1d)$$

3-PG calculates NPP (in Mg of dry matter per hectare per month, **1 Mg =  $1 \times 10^6$  g**) as constant fraction of gross primary productivity (GPP), using an NPP/GPP ratio ( $c_{\text{pp}} = 0.45 \pm 0.05$ , unitless) based on empirical evidence (Landsberg & Waring, 1997). In CARLUC, we convert from dry matter mass to carbon mass by assuming that carbon in forests is 50% of the dry mass. Recent work near Manaus suggests that the  $c_{\text{pp}}$  value in the Brazilian Amazon may be closer to 0.3 (Chambers *et al.*, in press). While our Monte-Carlo approach allows us to capture some of the uncertainty in this parameter, the implications of using a lower  $c_{\text{pp}}$  value are included in the Discussion section.

GPP is calculated by multiplying the amount of 'utilizable' absorbed photosynthetically active radiation (PAR) (uAPAR, moles of PAR per hectare per month) by an optimal quantum efficiency term ( $\alpha$ ) that represents the number of moles of carbon fixed per mole of uAPAR photons absorbed. The uAPAR is determined by the incident PAR at the top of the forest canopy ( $\text{PAR}_0$ ), by the amount of leaf area available to absorb the incident radiation (LAI), and by climatic and edaphic constraints on production, represented by the multipliers ( $f_i$  values ranging from 0 to 1) for the limitations imparted by soil water deficit defined by the ratio of the amount of water in the rooting zone to the maximum possible amount ( $\theta$ ), atmospheric vapor pressure deficit (VPD) and suboptimal temperature ( $T$ ), respectively. In the model, soil water depletion and VPD independently influence stomatal closure, and therefore productivity is limited by the more severe of the two constraints. Leaf area index (LAI, the total one-sided leaf surface area over a given square meter of land area, integrated from the ground to the top of the canopy) is predicted as a function of live leaf biomass multiplied by a single specific leaf area value (SLA, the area/mass ratio of foliage), and used to calculate the fraction of incident PAR absorbed by the forest canopy. PAR absorption is modeled using Beer's Law, assuming that a constant fraction of short wave radiation is

absorbed as it passes through a unit of LAI in the forest canopy. The Beer's Law coefficient is set at  $\lambda = 0.7$ , the default value for the 3-PG model, and close to the value ( $\lambda = 0.74$ ) used in a study of radiation use efficiency in the Amazon (Saldarriaga & Luxmoore, 1991). An average quantum efficiency of  $\alpha = 0.035$  was based on the literature (Landsberg & Waring, 1997). The factor 0.012 in Eqn (1b) is a conversion from moles of carbon fixed per  $\text{m}^2$  of land area to kilograms of carbon fixed per  $\text{m}^2$  of land area.

We use the same algorithms as 3-PG for calculating the SW deficit, VPD, and temperature constraints on NPP (Landsberg & Waring, 1997). We have not included limitation of productivity by fertility in the current version of the model because it is not clear how we could generate an appropriate soil fertility modifier for the entire Amazon. Recent measurements across the Amazon, including areas outside Brazil, suggest a relationship between stem growth and soil fertility (Malhi *et al.*, 2003), although it is not entirely clear whether this effect is due to limitations on gross productivity or to changes in allocation with soil fertility. If the effect is due to changes in allocation, it would be inappropriate to apply a modifier to productivity. A simple model for soil moisture is included to assess water limitation, using gridded precipitation data and the Penman–Monteith formulation for evapotranspiration directly from 3-PG. The soil moisture modifier is calculated as a function of the moisture ratio ( $r_{\theta}$ ), defined as

$$r_{\theta} = \frac{(\text{Current soil water content} + \text{water balance})}{(\text{Maximum available water})}. \quad (2)$$

Available water (mm) represents the maximum plant available water integrated over the entire rooting zone, which is dependent on the hydrological characteristics of the soil and the tree rooting depth. Water balance is the difference between precipitation and evapotranspiration over a month. Soil water can neither exceed the maximum available water nor fall below 0 mm.

We assume that all forests in the Amazon have access to a maximum of 5 m depth in the soil profile for water, in recognition of observations of deep roots in the Amazon (Nepstad *et al.*, 1994). The maximum rooting depth is spatially uniform in the model because controls on maximum rooting depth, while critical to understanding forest productivity and regional hydrology, are still poorly understood. Maximum plant-available soil water across the Amazon is based on the relationship between soil texture and water-holding capacity and has a spatial resolution of 8 km (Potter *et al.*, 1998). The soil water modifier,  $f_{\theta}$  is calculated as

$$f_{\theta} = \frac{1}{1 + [(1 - r_{\theta})/c_{\theta}]^{n_{\theta}}}. \quad (3)$$

3-PG requires four soil texture 'categories' (clay, clay-loam, sandy loam and sand) to calculate soil water modifier of primary production (Eqn (3)). The constants  $r_0$  and  $c_0$  have higher values for coarse vs. fine soils, reflecting the higher water potential in sand vs. clay for a given soil water content (Landsberg & Waring, 1997). We used previously derived soil texture categories (Potter *et al.*, 1998) that were based on clay content alone (FAO/UNESCO, 1971) and the soil texture triangle (Soil Survey Staff, 1990) to derive the four soil texture categories (Table 1). The soil texture dataset also has a grid size of 8 km × 8 km.

The 3-PG model reduces carbon fixation and evapotranspiration in response to atmospheric VPD using a negative exponential function (i.e.  $f_D = e^{-k \times \text{VPD}}$ ) to describe stomatal closure. The exponential coefficient ( $k$ ) determines the model's sensitivity to VPD. In these simulations  $k$  was assigned a value  $0.25 \text{ kPa}^{-1}$ , giving a good fit to measurements in a tropical forest (Granier *et al.*, 1995). SLA is set to a constant value of  $20 \text{ m}^2 \text{ kg}^{-1}$  of leaf carbon, similar to values observed in the Amazon (Carswell *et al.*, 2000) assuming that foliage is ~50% carbon by mass.

Rather than calculating the flux for each  $64 \text{ km}^2$  pixel in the model, we group the Amazon into 100 'productivity classes' based on the product of incident PAR and the climate modifiers included in Eqn 1(c). This product can be thought of as an index of how good the climate in a particular location is for growing plants. The classes are calculated by dividing the range of values into 100 bins. This aggregation leads to a substantial savings in the computation time needed to run the model for our model domain of ~76 000 model pixels.

We use the 1961–1990 monthly averaged precipitation and temperature datasets from East Anglia Climatic Research Unit CRU05 global climatology (New *et al.*, 1999) to drive the model (pixel size  $0.5^\circ \times 0.5^\circ$ ). The radiation data used in the model, including both PAR and total shortwave radiation, were produced as part of the NOAA/NASA Pathfinder project. Both datasets have a scale of  $0.5^\circ \times 0.5^\circ$  and temporal resolution of 1 month, averaged over the years 1990–1992. PAR is used to calculate primary productivity as the term  $\text{PAR}_0$  in Eqn (1d) and total shortwave radiation is used in the Penman Monteith calculation of evapotranspiration. These data are derived from ISCCP DX GOES data and an atmospheric radiation model (Pinker & Laszlo, 1992) and are available through the international large-scale biosphere–atmosphere experiment in the Amazon (LBA). We chose to take advantage of the higher resolution of the LBA radiation data ( $0.5^\circ$  vs.  $1^\circ$  for most radiation datasets), despite its relatively short duration.

**Table 1** Translation of soil texture categories to 3-PG/CARLUC categories

Previous texture category*	% Clay*	3-PG/CARLUC category (code)
Coarse	<20	Sand (1)
Coarse–medium	<30	Sandy/loam (2)
Medium	<48	Clay/loam (3)
Medium–fine	<67	Clay (4)
Fine	>67	Clay (4)
Lithosol		
Organic		Clay (4)

\*Potter *et al.* (1998).

3-PG, physiological principles in predicting growth; CARLUC, CARbon and Land-Use Change.

#### *Allocation of photosynthate and turnover rate of live carbon pools*

CARLUC uses 'lumped' live carbon pools to represent wood, foliage and fine root carbon for the entire forest stand (i.e., individual trees are not represented in the model). The fractional allocation coefficients of carbon between these three live biomass pools and their turnover times are fixed, as in the NASA-CASA model. Turnover of the three pools is modeled as a first-order loss process, with a characteristic turnover time for each pool. Our rationale is that existing data do not permit a more process-based modeling of the factors controlling allocation and turnover across the Amazon. Measurements of aboveground biomass accumulation during secondary succession in the Amazon also support the idea that aboveground biomass can be modeled assuming a constant turnover time over the entire course of forest re-growth (Salimon & Brown, 2000). We calculated the fractional allocation coefficients to match observed aboveground biomass and LAI at field sites near Manaus, where sufficient data are available (Honzak *et al.*, 1996; Roberts *et al.*, 1996; Nascimento & Laurance, 2002). These coefficients were then applied for all simulations across the entire Legal Amazon.

The size of the different carbon pools predicted for mature forests in the model depend on both the inputs into the pool (wood, leaves, etc.), and the transfer of carbon out of that pool. Therefore, if we are trying to match the observed LAI and aboveground biomass, the calculated fractional allocation coefficients will depend on our choices for the turnover times of the live biomass pools. We use the results from a study near Rio Branco, Acre State (Salimon & Brown, 2000) to estimate the turnover time of live wood. In that study, a simple curve of the form  $B(t) = B_0(1 - e^{-zt})$  was fit to measurements of standing aboveground biomass data during

secondary succession, yielding a turnover time of aboveground biomass ( $\alpha^{-1}$ ) of 40–65 years depending on the value of mature forest biomass ( $B_0$ ) used for the calculation. Consistent with this result, we chose a default value of  $50 \pm 5$  years for live wood turnover time. We chose an empirical approach to setting the wood turnover time because tree mortality is a stochastic process that is difficult to model. As discussed below in the Discussion section, ongoing field studies are now elucidating spatial patterns of biomass turnover and possible controlling variables. These relationships can be built into subsequent versions of the model. We also use a turnover time of foliage of  $12 \pm 6$  months (Roberts *et al.*, 1996), and a turnover time of fine roots of  $12 \pm 6$  months, which is consistent with values in the literature (Gill & Jackson, 2000).

To calculate aboveground biomass in CARLUC, we assume that roughly 80% of wood in the model lies aboveground, and 20% belowground, consistent with the choice made by Houghton *et al.* (2000) and resulting in an aboveground/belowground biomass ratio consistent with forest measurements (Enquist, 2002). As constraints, we use a value of  $178 \text{ MgC ha}^{-1}$  for live aboveground biomass (Nascimento & Laurance, 2002) and an LAI value of 5.7 (Roberts *et al.*, 1996). Allocation to fine roots is calculated as  $1 - P_w - P_f$ , where  $P_w$  is the fractional allocation to wood, and  $P_f$  is the allocation to foliage. Using our 'best guess' estimates for the turnover time of foliage and wood, the following fractional allocation coefficients yield agreement with measured aboveground biomass and LAI near Manaus: 0.25 of NPP to foliage, 0.40 to wood and 0.35 to fine roots. We vary the resulting fractional allocation coefficients by  $\pm 10\%$  (i.e. the fraction to foliage is  $0.25 \pm 0.025$ ) in the Monte-Carlo uncertainty study (see below) to explore the impact of uncertainty in the allocation coefficients on forest biomass and land-use fluxes. The fractional allocation coefficients in CARLUC are not varied with stand age or resource availability. Evidence for allocation changes with stand age in tropical forests is lacking. As mentioned above, the relationship between soil fertility and allocation between aboveground and belowground forest components is becoming clearer (Malhi *et al.*, 2003). In the future, experimental evidence for ecological relationships between environmental factors or stand development and carbon allocation will be incorporated into the model.

#### CARLUC soil carbon submodel

Decomposition of dead organic matter is based on the Roth-C Model (Jenkinson, 1990). As in Roth-C, we consider four components of soil organic matter (SOM):

a quickly decomposed metabolic fraction, a more recalcitrant structural component, a slow turnover humic fraction, and inert organic carbon, representing elemental carbon or organic carbon that is chemically or physically protected from decomposition and has a turnover time exceeding 50 000 years. However, we have simplified Roth-C by using fixed first-order decomposition rates, and added a woody debris pool. Thus, in the current version of the model, we do not account for the impact of changes in soil climate on soil carbon dynamics.

Based on a recent study of soil carbon isotopes in a Paragominas ( $2^\circ 59'S$ ,  $47^\circ 31'W$ ) Oxisol (Trumbore *et al.*, 1995), litter inputs are assumed to be 10% 'fast cycling' metabolic material with a turnover time of  $<1$  year, and 90% 'slow cycling' structural material, with a turnover time of 4 years. Soil humus is given a turnover time of 25 years and the inert organic matter (IOM) pool is assigned a radiocarbon isotopic signature of  $-993\%$ . The fraction of litter that passes to humus rather than being mineralized to  $\text{CO}_2$  and the size of the IOM pool are then calculated, which yield the best agreement with the observed carbon storage ( $25.7 \text{ kgC m}^{-2}$ ) and bulk radiocarbon signature ( $-557\%$ ) measured to a depth of 8 m in 1992 (Trumbore *et al.*, 1995). The optimization was performed off-line in the software package VENSIM ([www.vensim.com](http://www.vensim.com)), using fixed litter input rates in a version of the decomposition submodel that includes carbon isotopes. To incorporate  $^{13}\text{C}$  and  $^{14}\text{C}$  into the model, each year's foliar and fine root detrital inputs were 'labeled' with the atmospheric radiocarbon signature of the input year, using atmospheric data from 1950 to the 1990s for the Southern Hemisphere (Manning & Melhuish, 1994) and the INTCAL-2000 (Stuiver *et al.*, 1998) dataset for the 10 000 years before 1950. We assume that the input of carbon from surface litter and root detritus each year is a constant  $1.2 \text{ kgC m}^{-2}$ , which balances the portion of soil respiration arising from SOM decomposition, which Trumbore *et al.* (1995) state is roughly one half of total soil respiration ( $2400 \text{ gC m}^2 \text{ yr}^{-1}$ ). We also assume that fine root and leaf litter have the same proportions of metabolic and structural material. Coarse woody debris is considered separately from fine litter, with a single first-order coarse woody debris decomposition rate of 0.17 per year (Chambers *et al.*, 2000).

While we simulate the size of the IOM pool is necessary for the optimization, because of the strong influence it exerts on the bulk radiocarbon value, we do not explicitly simulate the dynamics of the IOM pool in CARLUC. Instead, we assume that the IOM pool will not be affected by changes occurring on a decadal time scale. This choice is consistent with the operation of the

original Roth-C model. Therefore, none of our results includes carbon stored in the IOM pool. We do simulate the generation of charcoal during deforestation, which is considered inert in the model, but distinguish it from IOM, which has accumulated over millennia.

Using the Trumbore *et al.* (1995) measurements, we calculate a humification coefficient of 0.17 (the fraction of decomposed organic matter that passes to humus rather than CO<sub>2</sub>) and an IOM pool size of 15.2 kgC m<sup>-2</sup> (~60% of the total carbon stock). The value we calculate for the humification coefficient is close to the Roth-C model value (Jenkinson, 1990), which is based on the <sup>14</sup>C labeling studies of Sorenson ( $F_h = 0.15$ ). While we do not expect the value to be exactly the same in tropical soils, we are confident that the humification coefficient is biologically plausible. The size of the IOM pool is consistent with the value derived from the radiocarbon analysis in Trumbore *et al.* (1995). The model is able to match both the total carbon storage and bulk isotopic signature to a depth of 8 m in the soil, measured in 1992. During production runs, all of the litter and soil pools are initialized at zero, and the model is run to steady state before any land-use changes are initiated. Litter inputs during the production runs are calculated as a function of leaf, wood and root turnover.

#### *Disturbance carbon flows*

During deforestation for agriculture (crops or pasture), we assume the same fate for ecosystem carbon pools as Houghton *et al.* (2000), with 20% of the initial above-ground forest biomass (including coarse woody debris generated by the undisturbed forest) combusted to CO<sub>2</sub>, 70% left as slash, 8% removed to wood products and 2% converted to elemental carbon. We also assume that the entire litter layer is combusted to CO<sub>2</sub> during burning. The wood products pool is assumed to decay with a time constant of 10 years, as in Houghton *et al.* (2000).

#### *Land-cover dynamics*

The annual rate of primary forest clearing from 1988 to 1998 for the entire Brazilian Amazon, as determined by the Brazilian Space Agency (INPE) by inspection of Landsat imagery, is taken from Table 1 in Houghton *et al.* (2000). We lower this rate by 12.5% to account for the discrepancy between the INPE rate and the rate calculated by Houghton *et al.* (2000) from digital Landsat MSS imagery. The deforestation rate is given an uncertainty value of ± 12.5% to cover the range between the two estimates. The average rate for the period 1978–1988, taken from the literature, is derived

from remote sensing imagery (Skole & Tucker, 1993), while we use the annual rate from the FAO for 1970–1978 (as cited in Skole & Tucker, 1993).

The spatial pattern of deforestation is mapped by identifying all of the pixels that are classified as cleared land or secondary forest in the 1986 and 1992 TRFIC land-cover classification images (resolution of 57 m). We then use the high-resolution imagery to calculate the fraction of each 64 km<sup>-2</sup> CARLUC pixel that has experienced deforestation and assume that the same fraction of annual deforestation occurs in each pixel in each year. Since each pixel is associated with a certain productivity class (see the section on Forest productivity modeling, above for the definition of productivity class), we can calculate the fraction of the total deforested area that lies in each productivity class. This step is necessary because different productivity classes have different responses to land-cover change. We assume that the spatial pattern of abandonment is the same as the pattern of deforestation.

#### *Annual net carbon flux calculation*

The annual net carbon flux due to deforestation and forest re-growth is calculated using an ‘impulse-response’ approach (Thompson & Randerson, 1999). In our study, the ‘impulse’ corresponds to the sudden shifts in the carbon cycle model that occur during land-cover change. The ‘response’ is the re-equilibration of the model carbon fluxes after the land-cover change. For example, when primary forest is cleared, there is an immediate release of carbon due to combustion of the downed trees and litter, and a slower release due to decomposition of the remaining slash and stored soil carbon. An area that is released from agriculture to secondary forest will begin accumulating forest carbon through primary productivity, which then passes through the ecosystem to the detritus and soil carbon pools. The flux response curves will vary with productivity class, but we assume that forest recovery is not hindered by multiple cycles of clearing and re-growth. To calculate a flux response curve, CARLUC generates an ensemble of 100 carbon storage response curves for each of the 100 productivity classes, using a Monte-Carlo approach. In the Monte-Carlo approach, each parameter and input in the CARLUC model is given a mean value and a standard deviation representing the parameter’s uncertainty, and assumed to have a normal distribution (Table 2). The first derivative of each carbon storage curve in the statistical ensemble is a carbon flux response curve. The annual mean carbon flux response curve and the standard deviation are then calculated from the ensemble of monthly flux curves.

**Table 2** Parameters used in the CARLUC Model

Parameter	Description	Value mean $\pm$ error term
$c_{pp}$	NPP/GPP ratio	0.45 $\pm$ 0.05 (dimensionless)
$\alpha$	Quantum efficiency	0.035 $\pm$ 0.005 (mol C (mol uAPAR) <sup>-1</sup> )
SLA	Specific leaf area	20 $\pm$ 5 (m <sup>2</sup> (kg leaf C) <sup>-1</sup> )
$P_w$	Fractional allocation to wood	0.4 $\pm$ 0.04 (dimensionless)
$P_f$	Fractional allocation to foliage	0.25 $\pm$ 0.025 (dimensionless)
$P_r$	Fractional allocation to fine roots	0.35 $\pm$ 0.035 (dimensionless)
$F_h$	Fraction of decomposed dead organic matter passing to humus	0.17 $\pm$ 0.017 (dimensionless)
$F_m$	Metabolic/structural ratio in leaves and roots	0.1 $\pm$ 0.01 (dimensionless)
PAR <sub>0</sub>	Incident photosynthetically active radiation above the forest	Model input (MJ m <sup>-2</sup> month <sup>-1</sup> )
$\lambda$	Fractional absorption of PAR by foliage	0.7 (per unit LAI)
$\tau_w$	Turnover time of live wood	600 $\pm$ 60 (months)
$\tau_f$	Turnover time of live leaves	12 $\pm$ 6 (months)
$\tau_r$	Turnover time of live roots	12 $\pm$ 6 (months)
$\tau_m$	Turnover time of the metabolic fraction of leaf and root litter	4 $\pm$ 0.4 (months)
$\tau_s$	Turnover time of the structural fraction of leaf and root litter	48 $\pm$ 4.8 (months)
$\tau_h$	Turnover time of soil humus carbon	300 $\pm$ 30 (months)
$\tau_{wd}$	Turnover time of woody debris	60 $\pm$ 6 (months)
$\tau_{wp}$	Turnover time of wood products	120 (months)

CARLUC, CARBON and land use change; NPP, net primary productivity; GPP, gross primary productivity.

We use a convolution sum to calculate the net flux due to deforestation and secondary forest growth in a given year (e.g., 1980) by adding together the flux contributions of land-cover changes that occurred in preceding years (e.g., 1970–1980). The following equation is used for this purpose:

$$F(t) = \sum_{i=1}^{100} \sum_{\tau=1}^{29} f(i) \times a(t - \tau) \times R(i, \tau). \quad (4)$$

In Eqn (4),  $F(t)$  is the net carbon flux due to land-cover change in year  $t$  ( $t = 1970$ – $1998$ ) for the entire Brazilian Amazon in PgC yr<sup>-1</sup> due to the contribution of land-cover change that occurred from 1970 until year  $t$ . The factor  $f_i$  is the fraction of the land-cover change in productivity class  $i$ . The product of  $a(t - \tau)$  and  $R(i, \tau)$  summed over  $\tau$  is a convolution of the annual area ( $a$ ) experiencing a given land-use change  $\tau$  years before year  $t$ , and the flux response curve ( $R$ ) of productivity class  $i$  to that land-use change with time ( $\tau$ ) since it occurred.

#### Uncertainty in the annual net carbon flux

Each of the terms in Eqn (4) has an associated uncertainty. To estimate the precision of our calculated flux due to land use and re-growth, we propagate all of the uncertainties in our approach. The fraction of deforestation or abandonment in each productivity class is given a nominal uncertainty of  $\pm 10\%$ , since

there was no error analysis of the land-cover classifications included with the TRFIC land-cover maps. The area of primary forest cleared or abandoned each year is given an uncertainty of 25% ( $\pm 12.5\%$ ), reflecting the discrepancy between the INPE estimate and an estimate derived from a Landsat MSS-based land-cover classification for 1988 (Houghton *et al.*, 2000). The resulting uncertainty in the carbon flux response curve is generated using a Monte-Carlo approach described previously.

#### Sensitivity analysis

We use an equation from Friend *et al.* (1993) to calculate the sensitivity ( $\beta'$  factor) of the steady-state carbon storage to each model parameter and input, using the following equation:

$$\beta = (C_{+10} - C_{-10})/C_{\text{default}}. \quad (5)$$

$\beta$  is the sensitivity factor,  $C_{\text{default}}$  is the steady-state carbon storage predicted by CARLUC using the best estimate for a given parameter (Friend *et al.*, 1993),  $C_{+10}$  is the steady-state carbon storage when the parameter is increased by 10%, and  $C_{-10}$  is the steady-state carbon storage with the parameter decreased by 10%. As a case study, we present the results of our sensitivity analysis using Rio Branco, Acre State ( $\sim 10$  S, 68 W), which is an LBA field site in SW Amazonia in an area undergoing rapid deforestation.

### Model experiments

We performed three experiments (Table 3) with the model. In the first experiment ( $H_0$ ), annual abandonment of agricultural land is 30% of the annual deforestation, and changes in fine litter and soil carbon pools are neglected, as in Houghton *et al.* (2000). The second experiment ( $H_{\text{soil}}$ ) assumes the same rate of agricultural abandonment, but includes aboveground and belowground fine litter and soil carbon as integral parts of the carbon cycle model. The third experiment ( $H_{\text{cluc}}$ ) includes litter and soil carbon pool changes, and uses a more dynamic pattern of land-cover change, simulating both agricultural abandonment and re-clearing of secondary forests, based on a time series of land-cover classification maps. As in Houghton *et al.* (2000), we do not simulate the production and cycling of pasture or crop carbon in any of the model experiments.

This more dynamic land-use change scenario in the  $H_{\text{cluc}}$  experiment was inspired by a study of land-cover dynamics using SPOT imagery (Alves & Skole, 1996) that documented high rates of both abandonment and re-clearing in Rondônia in the late 1980s. Re-clearing in the model is a dynamic within lands that have been identified as already having been deforested, and is not included in the INPE annual deforestation estimates, which only assess clearing of primary forest. The area that is cleared each year undergoes a repeated cycle in the  $H_{\text{cluc}}$  run: several years as agriculture, then abandonment and several years of growth as secondary forest, followed by re-clearing for another round of agriculture. The average lifetimes of agricultural land and secondary forest are calculated to match the time series of total cleared area across the Legal Amazon in the 1986, 1992 and 1996 TRFIC land-cover classification maps. The best results are obtained if land spends roughly 7 years as agriculture and 7 years as secondary forest. However, the time spent as agriculture or re-

growing forest is randomly varied in the Monte-Carlo simulations by  $\pm 2$  years (1SD), in order to include the uncertainty in these parameters in our estimation of the net flux. Maintenance of agricultural land is simulated as additional rounds of slash and burning every 2 years (Uhl *et al.*, 1988) on cleared land. In the future, other statistical distributions of land tenure should be tried as more evidence becomes available (for example, if half of the land was abandoned after 2 years and half abandoned after 12 years). Here, we have taken the simplest case that is consistent with the time series of land cover based on the satellite imagery, in order to study the sensitivity of the net flux across the Amazon basin to very different assumptions about land tenure.

For the  $H_0$  and  $H_{\text{soil}}$  experiments, we use Eqn (4) to separately calculate the release of carbon caused by deforestation, and the net accumulation during secondary re-growth. These fluxes are calculated by convolving the time series of annual deforestation and abandonment rates with the corresponding flux response curves. The land-cover changes in the  $H_{\text{cluc}}$  experiment are too complex to separate into different parts, so we convolve the time series of annual deforestation with the flux response curve corresponding to the repeated cycle of clearing and abandonment used in the  $H_{\text{cluc}}$  case. This approach yields a net flux that represents a combination of disturbance and recovery fluxes.

## Results

### *The net flux due to deforestation and re-growth*

The net flux due to deforestation and re-growth from 1970 to 1998 for experiment  $H_0$  (Fig. 2a) has a shape similar to the results of the Houghton *et al.* (2000) study. The net flux (line A) is the sum of gross flux due to deforestation (B) and the net re-growth flux on abandoned land (C). The net flux reaches a maximum in 1990 of  $0.35 \text{ PgC yr}^{-1}$ , with an uncertainty of  $\sim 35\%$ . The magnitude of the net flux predicted by CARLUC is higher than the net flux presented in Houghton *et al.* (2000) over the entire period 1970–1998. The re-growth flux is similar to the Houghton *et al.* (2000) result, reaching a maximum uptake of  $\sim 0.06 \text{ PgC yr}^{-1}$  by 1998, so that most of the difference is due to the impact of the higher mature forest biomass predicted by CARLUC on the deforestation flux. We also show a time series of the total carbon storage on land classified as cleared or secondary forest in the 1986 and 1992 TRFIC maps (Fig. 2b) from 1970 to 1998, excluding humus and litter pools because of the assumptions of the  $H_0$  experiment. The total carbon storage (line A) is the sum of two terms: the carbon stored on undisturbed

**Table 3** Model experiments included in the paper

Experiment	Description
$H_0$	Annual abandonment = $0.3 \times$ annual deforestation; no re-clearing of secondary forest; changes in litter and soil carbon not considered
$H_{\text{soil}}$	Annual abandonment = $0.3 \times$ annual deforestation; no re-clearing of secondary forest; litter and soil carbon included as integral part of the carbon cycle model
$H_{\text{cluc}}$	Abandonment and re-clearing more mechanistically modeled; litter and soil carbon included in the model

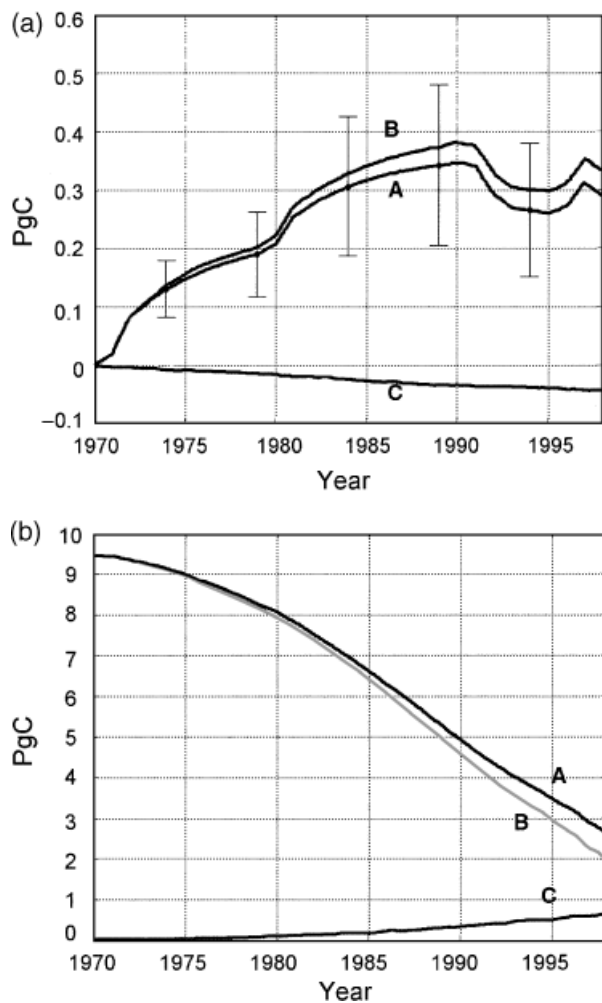


**Fig. 2** (a) Time series of the net carbon flux due to deforestation and forest re-growth from 1970 to 1998 (A), shown as the sum of the flux due to deforestation (B) and the flux due to re-growth (C), for the  $H_0$  experiment. (b) Time series of total carbon stored on land classified as cleared or re-growing in the 1986 and 1992 Tropical Rainforest Information Center (TRFIC) maps (A), the sum of carbon stored on undisturbed land plus slash remaining after deforestation (B) and carbon stored due to secondary forest re-growth (C). Results are from the  $H_0$  experiment.

areas plus the slash created by deforestation that has not decomposed (line B) and the carbon re-accumulating in secondary forests (line C). The time series of carbon storage shows that between 1970 and 1998, the net flux due to deforestation and re-growth caused a total net release of 6.8 PgC to the atmosphere. The net carbon release from 1989 to 1998 is 2.8, 1 PgC higher than the average cited in Houghton *et al.* (2000). A typical flux response curve, representing the average of 100 Monte-Carlo runs, is shown for the  $H_0$  case, for the deforestation flux (Fig. 3a), and the re-growth flux (Fig. 3b). The deforestation flux for the  $H_{\text{soil}}$  experiment (not

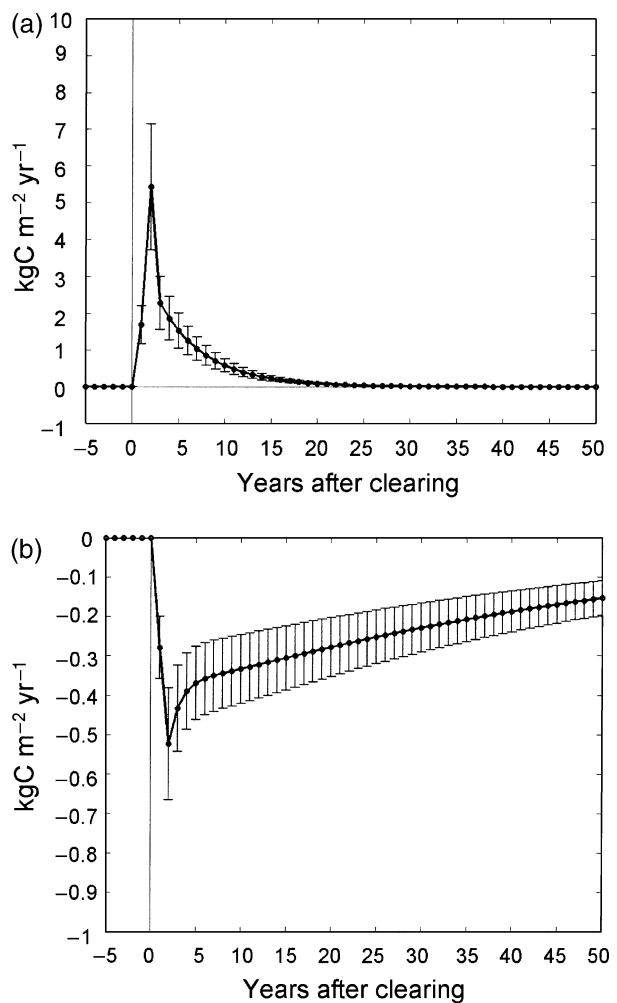


**Fig. 3** (a) Flux response curve used to calculate carbon release due to combustion and decomposition with time after land is cleared in the  $H_0$  and  $H_{\text{soil}}$  experiments, for a representative productivity class. (b) Flux response curve used to calculate carbon uptake during secondary forest growth in the  $H_0$  and  $H_{\text{soil}}$  experiments, for a representative productivity class.

shown) has a longer decay time because it includes soil humus, which has a longer turnover time.

The net carbon flux predicted by the other model experiments,  $H_{\text{soil}}$  (line B in Fig. 4) and  $H_{\text{Icluc}}$  (line C) is similar to the  $H_0$  case (line A), despite large differences in the model configuration. The difference between lines A and B in Fig. 4 shows the impact of including litter and humus pools in the model, while the difference between lines B and C shows the impact of different treatments of land-use change. The  $H_{\text{soil}}$  experiment always predicts higher fluxes than the  $H_0$  experiment, and in the late 1980s, the difference reaches  $\sim 0.05 \text{ PgC yr}^{-1}$ . The differences between  $H_{\text{soil}}$  and  $H_{\text{Icluc}}$  are more complex, with the  $H_{\text{Icluc}}$  flux falling

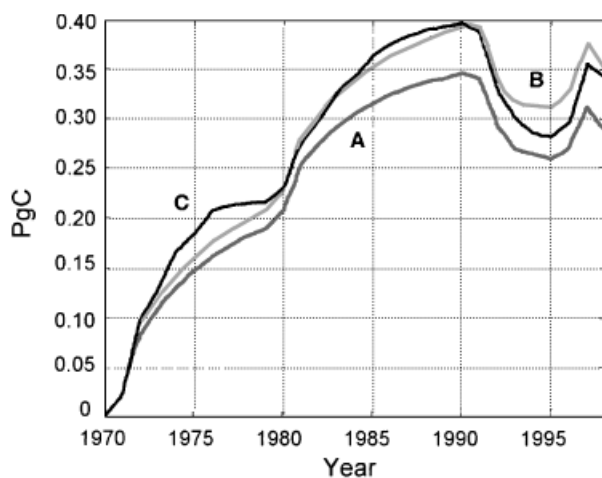


Fig. 4 The time series of the net flux for the three experiments:  $H_0$  (A),  $H_{soil}$  (B) and  $H_{lcluc}$  (C).

below the  $H_{soil}$  flux around 1990. The flux response curves used in the  $H_{soil}$  case are similar to those used in the  $H_0$  case; however, we show a typical flux response curve used in the  $H_{lcluc}$  experiment for comparison (Fig. 5). In the  $H_{lcluc}$  flux response curve, which is an average of 100 Monte-Carlo simulations, there are three initial spikes, corresponding to the initial clearing and maintenance burning, and then cycles of carbon uptake and release corresponding to abandonment and re-clearing. The spikes in the flux that occur during subsequent rounds of re-clearing are smoothed because we vary the lifetime of cleared land in the Monte-Carlo simulations, and the different Monte-Carlo runs are averaged. The release of carbon from 1970 to 1998 is the same for the  $H_{soil}$  and  $H_{lcluc}$  experiments, totaling 7.8 PgC, which is about 1 PgC higher than the  $H_0$  experiment for this time period.

#### Steady-state ecosystem carbon storage

Modeled total steady-state ecosystem carbon storage in Amazonia, including all carbon pools except for IOM, ranges from 170 to 340 MgC ha<sup>-1</sup>, with a mean value of 285 MgC ha<sup>-1</sup>, generally decreasing from north to south. Total live biomass, including live leaf, wood and fine root pools, shows the same geographical pattern, but the values range from 120 to 240 MgC ha<sup>-1</sup> (mean 202 MgC ha<sup>-1</sup>), while carbon storage in above-ground live biomass, assuming 80% of wood is above-ground, ranges from 93 to 189 MgC ha<sup>-1</sup> (mean 159 MgC ha<sup>-1</sup>). We show a map of total live biomass (Fig. 6), including wood, leaves and fine roots, for comparison with the maps included in a recent review of Brazilian Amazon biomass estimates (Houghton *et al.*, 2001). The forest/nonforest mask in this figure

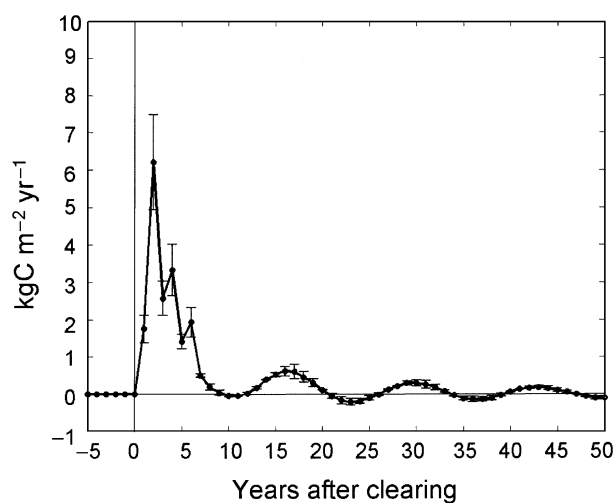


Fig. 5 The flux response curve for the  $H_{lcluc}$  experiment combining both uptake and release terms and including both abandonment and re-clearing.

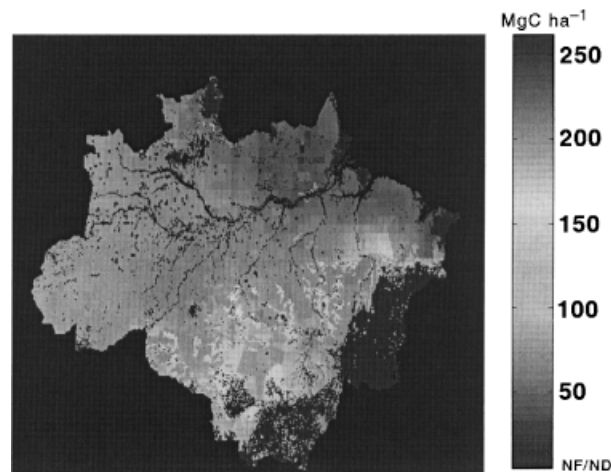


Fig. 6 A map of total live biomass (wood + leaves + fine roots) for mature forests in the Legal Amazon, calculated by the CARLUC (for CARbon and land-use change) model. NF/ND refers to nonforest pixels, or pixels with missing data in the forest/nonforest mask.

is derived from NOAA AVHRR imagery (Stone *et al.*, 1994), with nonforest areas (mainly savanna) shown in dark gray. The average total live biomass (i.e., not including woody debris) of 202 MgC ha<sup>-1</sup> lies toward the high end of the range between the low (130 MgC ha<sup>-1</sup>) and high (210 MgC ha<sup>-1</sup>) estimates based on RADAMBRASIL surveys in Houghton *et al.* (2000). Comparison of predicted and measured above-ground live biomass carbon from 22 sites in the Brazilian Amazon (Houghton *et al.*, 2001) showed no significant difference (observed = 148 ± 43 MgC ha<sup>-1</sup>;

modeled =  $161 \pm 11 \text{ MgC ha}^{-1}$ , error term = standard deviation of the means).

The influence of soil water limitation on steady-state carbon storage in the model is evident in the drier transitional forest in eastern and southern Amazonia. The total live biomass (leaves, wood and fine roots) for deforested areas averages  $147 \text{ MgC ha}^{-1}$ , which is only 73% of the predicted average value for the entire Legal Amazon, because deforestation is concentrated in these drier regions, along roads in the 'arc of deforestation and forest disturbance' (Nepstad *et al.*, 2001).

Total ecosystem carbon storage is dominated in all regions by the carbon in tree stems due to the long turnover time of this carbon pool and the relatively high flow of carbon into the pool via NPP. The partitioning of ecosystem carbon storage for a pixel near Manaus at steady state shows the majority of total carbon storage in stem wood, on the order of 60%, assuming 80% of wood is aboveground. The uncertainty of the steady-state biomass, derived using the Monte-Carlo technique, is roughly 35% of the mean value (1 SD).

#### Model sensitivity

The CARLUC model is most sensitive to the factors that determine the storage of carbon in wood: factors that affect net primary production (radiation, light use efficiency, fraction of gross photosynthesis going to respiration), factors that decide the fraction of NPP going to wood and the turnover time of wood (Fig. 7). This sensitivity to storage in wood arises because that carbon pool has a large input and long turnover time, and thus has a high capacity to store carbon, as has been noted elsewhere (Chambers *et al.*, 2001). The soil carbon submodel parameters have little effect on the predicted ecosystem carbon storage. The reason is that relatively little carbon is passed to the soil pools, and the turnover times are relatively fast, leading to small amounts of carbon storage. The most surprising result of the steady-state carbon storage sensitivity testing is the sensitivity to maximum temperature in the model. While temperature has little direct effect on plant production in the model (the temperature in the Amazon is ideal for plant growth), maximum temperature has a large indirect effect through the soil moisture budget. If maximum temperature is increased by 10% in the model (a large increase in mean annual temperature of roughly  $3^\circ\text{C}$ ), VPD in the model increases disproportionately because of the nonlinear relationship between temperature and saturated vapor pressure. Increased VPD has a small direct effect on photosynthesis due to decreased stomatal conductance. However, high VPD also leads to faster soil water

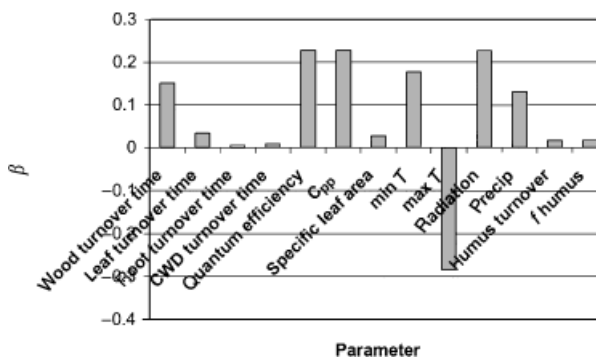


Fig. 7 The sensitivity of mature forest biomass to different model parameters in CARLUC (for CARbon and Land-Use Change), shown for Rio Branco, Acre State.

depletion due to evapotranspiration. In areas with seasonal drought, increased soil water deficit leads to decreased NPP in the model. Therefore, inaccurate temperature inputs could lead to biases in the model predictions.

#### Discussion

##### Carbon flows in mature forests – comparison with independent data

We calibrated fractional allocation in the model using a single site near Manaus, based on observed mature forest LAI and aboveground biomass. To check that the model is accurate in other sites, and for processes that were not considered in the calibration, we compare the predictions made by the model for aboveground biomass, annual stem growth, litterfall and coarse woody debris with measurements made by different LBA-Ecology teams in the FLONA Tapajos (approximately  $2.9^\circ\text{S}$ ,  $55^\circ\text{W}$ ). The CARLUC model, using the CRU05 climatology, predicts mature forest aboveground carbon storage in live tree biomass of  $180 \text{ MgC ha}^{-1}$ , annual aboveground stem growth of  $3.6 \text{ MgC ha}^{-1} \text{ yr}^{-1}$ , annual litterfall of  $2.8 \text{ MgC ha}^{-1} \text{ yr}^{-1}$  and steady-state coarse woody debris of  $22 \text{ MgC ha}^{-1}$  at FLONA Tapajos.

Measurements of aboveground live biomass include:  $197 \text{ MgC ha}^{-1}$  (1984 IBAMA survey, Miller *et al.*, 2003),  $185 \text{ MgC ha}^{-1}$  (2000 TREVISIO survey, Miller *et al.*, 2003) and  $132 \text{ MgC ha}^{-1}$  (range 79–209, Keller *et al.*, 2001) at the km 83 site (includes corrections for small trees, vines and epiphytes);  $145.3 \pm 5.7$  (Rice *et al.*, 2003) in live trees  $> 10 \text{ cm}$  diameter at breast height (dbh) at the km 67 site in 2001;  $152.5 \text{ MgC ha}^{-1}$  (Nepstad *et al.* 2002) in trees  $\geq 10 \text{ cm}$  dbh and lianas  $\geq 5 \text{ cm}$  diameter in the control plot at the Seca Floresta experiment. Therefore, the model result for aboveground live biomass in trees

is toward the upper end of the range of observations, which range from about 130 to 200 MgC ha<sup>-1</sup>. The comparison is a bit complicated in that we did not consider lianas and epiphytes, while some of the biomass inventory measurements did not consider small trees. Our prediction of CWD (22 MgC ha<sup>-1</sup>) is in line with measurements at Tapajos. Rice *et al.* (2003) found that fallen coarse woody debris >10 cm totaled 23.3 ± 6.1 MgC ha<sup>-1</sup>.

Our prediction of aboveground carbon accumulation in live stems (3.6 MgC ha<sup>-1</sup> yr<sup>-1</sup>) is higher than measured values. Measurements include 2.9 MgC ha<sup>-1</sup> yr<sup>-1</sup> in trees ≥10 cm dbh at the Seca Floresta control plot (Dr Daniel Nepstad, unpublished data) based on 2.5 years of measurements and 3.28 ± 0.23 MgC ha<sup>-1</sup> yr<sup>-1</sup> at the km 67 site (Rice *et al.*, 2003), also in stems ≥10 cm dbh. Measurements at the km 83 site are similar to the km 67 results (Goulden *et al.*, 2003). It is unclear what proportion of carbon accumulation is occurring at these sites in stems <10 cm dbh, but accounting for these small trees would increase these estimates of annual wood growth. Our prediction can also be compared with the 3.4 MgC ha<sup>-1</sup> yr<sup>-1</sup> we derived by a linear regression of the Zarin *et al.* (2001) data of aboveground biomass vs. age (see below), assuming that the majority of aboveground biomass accumulation in re-growing stands goes into wood.

Compared with Tapajos measurements, the model (2.8 MgC ha<sup>-1</sup> yr<sup>-1</sup>) underestimates litterfall. Four years of measurements in the Seca Floresta control plot yield an average annual fine litterfall rate of about 3.3 MgC ha<sup>-1</sup> yr<sup>-1</sup>, including foliage, fruits, seeds, flowers and twigs <1 cm diameter (Dr Daniel Nepstad, unpublished data). Measurements at the km 67 site total 3.96 MgC ha<sup>-1</sup> yr<sup>-1</sup> in leaves and 5.74 MgC ha<sup>-1</sup> yr<sup>-1</sup> if fruit, flowers and twigs <2 cm diameter are included (Rice *et al.*, 2003). Litterfall at the km 83 site totals 3.1 MgC ha<sup>-1</sup> yr<sup>-1</sup>, counting only leaves (A.M.S. Figueira, unpublished data). An underestimation of litterfall can be explained by the value we chose for SLA. We chose a value of 10 cm<sup>2</sup> (gDW)<sup>-1</sup> (20 cm<sup>2</sup> gC<sup>-1</sup>) from the literature, while measurements at the km 83 site (A.M.S. Figueira, unpublished data) suggest the value is somewhat lower, roughly 8.7 cm<sup>2</sup> g<sup>-1</sup>. Therefore, the model allocates less carbon to foliage when matching the observed LAI at the ZF2 site in Manaus during the model calibration. If we used an SLA of 8.7, litterfall would be 3.2 MgC ha<sup>-1</sup> yr<sup>-1</sup>. Slight biases in predicted leaf biomass and litterfall will cause only small inaccuracies in our results, because they represent small carbon pools in the model. Small biases in LAI will also have little impact on forest productivity because at LAI > 5, 97% of incident PAR is absorbed.

A final comparison involves GPP, which is underestimated by the model (24.7 MgC ha<sup>-1</sup> yr<sup>-1</sup>, using the Pathfinder PAR data) compared with an estimate based on eddy covariance measurements at the km 83 site (~30 MgC ha<sup>-1</sup> yr<sup>-1</sup>, Miller *et al.*, 2003). This underestimate is balanced by our model value of the forest carbon use efficiency ( $c_{pp}$ ), which may be higher than the true tropical forest value, as mentioned above (see Chambers *et al.*, in press), so that our predicted NPP is less biased than GPP. Our underestimate of GPP may be caused by our choice of canopy quantum efficiency. The gridded Pathfinder PAR dataset gives a radiation input of 7417.5 mol PAR m<sup>2</sup> yr<sup>-1</sup>. Dividing 30 MgC ha<sup>-1</sup> yr<sup>-1</sup> (measured GPP) by this radiation input, after converting to the proper units, gives a canopy quantum efficiency of 0.034 mol C fixed per mole radiation utilized, assuming that all radiation is absorbed and utilized by the canopy. However, it is likely that not all incoming PAR is absorbed and utilized by leaves. Some falls on nonphotosynthetic components (including the forest floor), and some may not be utilized because of environmental limitations on photosynthesis such as high VPD. Therefore, the true canopy radiation use efficiency may be higher than our model value of 0.036. For comparison, the GLO-PEM model (Prince & Goward, 1995) predicts a higher canopy quantum efficiency ( $\alpha = 0.04$ ) at 26 °C. Comparison with seasonal variation in NEE would be instructive, but until we include sensitivity of soil and litter decomposition to variability in soil climate, the comparison is not meaningful. We used fixed turnover times in the decomposition submodel because we were interested in long-term changes in ecosystem carbon storage.

What have we learned from the comparison between model predictions and measurements at the FLONA Tapajos? Allocation to wood is too high in the model, unless including stem growth in stems <10 cm in the measurements is significant. A smaller allocation to wood would require a longer residence time for wood to match the observed aboveground living biomass carbon storage. A longer residence time in wood would still be consistent with the range of estimates from the Salimon & Brown (2000) study, and also with basin-wide measurements that show increasing turnover time with decreasing stem growth, such that forests accumulating less than 3 MgC ha<sup>-1</sup> yr<sup>-1</sup> in stems have turnover times >50 years (Malhi *et al.*, 2003). In addition, we will use a lower value of SLA in the future, which will have the effect of raising the fraction of photosynthate allocated to leaf production and simulated litterfall. We will also likely use a higher value for the canopy quantum efficiency and a lower value of carbon use efficiency, so that we can be more consistent with observed GPP and yet account for

measurements indicating that carbon use efficiency is lower in tropical forests than in temperate forests, while not causing biases in NPP. The range in observed aboveground biomass does not make this a very strong constraint on the model; however, it is encouraging that our estimate lies within the observed range. Lastly, there are significant amounts of carbon cycling through tropical ecosystems in forms not simulated by the model, such as lianas, small twigs, flowers and fruit. The absence of these carbon pools in the model make comparison with measurements more difficult, as does the lack of measurement of the smallest diameter classes in the forest.

Perhaps the most important point to be learned from the model/observation comparison is the necessity to consider as many ecological processes as possible in the initial model calibration. We initially focused on mature forest biomass because this is the major control on the carbon released by deforestation, and we predict aboveground live biomass consistent with the observations. However, it is possible to get the right amount of carbon storage with offsetting errors in the inputs into a carbon pool and the turnover of that pool. Our comparison with observations at FLONA Tapajos is helpful in improving our understanding of the mechanisms controlling steady-state carbon storage in these forests.

#### *Recovery of aboveground carbon in secondary forests*

We use data included in a recent synthesis study of aboveground biomass accumulation in re-growing Amazonian forests (Zarin *et al.*, 2001) to predict aboveground carbon storage after 20 years of re-growth in Amazon for comparison with CARLUC. We fit a line to a graph of aboveground biomass vs. stand age for nonsandy sites, pinning the intercept at  $0 \text{ MgC ha}^{-1}$ , and multiplying the slope by 0.5 (ratio of carbon to dry weight of biomass) to get aboveground carbon accumulation. The resulting best-fit line has an  $R^2$  value of 0.6 and a slope of  $3.4 \text{ MgC ha}^{-1} \text{ yr}^{-1}$ . Based on this simple model, a 20-year-old forest will have live aboveground biomass carbon storage of roughly  $68 \text{ MgC ha}^{-1}$ . CARLUC predicts accumulated aboveground carbon near Manaus after 20 years of  $60 \text{ MgC ha}^{-1}$ , slightly lower than predicted by the stand age-carbon storage relationship derived from the data, and much lower than the  $100 \text{ MgC ha}^{-1}$  predicted using the algorithms from the Houghton *et al.* (2000) study. By comparison, the relationship between aboveground biomass and GSDY, a heat sum index described in Zarin *et al.* (2001), predicts aboveground carbon storage of  $95 \text{ MgC ha}^{-1}$  for nonsandy soil near Manaus, assuming that forest biomass is 50% carbon. We predict

carbon storage as a function of stand age as well as GSDY because, for the sites presented in Zarin *et al.* (2001), GSDY is highly correlated with stand age ( $R^2 = 0.98$ ). None of the unexplained variance of the relationship between aboveground biomass and stand age is explained by climate, using the GSD values included in the paper. Therefore, we conclude that it is equally valid and simpler to predict biomass accumulation using stand age for the sites they present.

Uhl *et al.* (1988) found that the relationship between stand age and aboveground biomass varied with prior land-use intensity. CARLUC predicts  $49 \text{ MgC ha}^{-1}$  for a 20-year-old forest in Paragominas, while the empirically derived equations predict  $115.5 \text{ MgC ha}^{-1}$  under light-intensity prior land use, and  $45.5 \text{ MgC ha}^{-1}$  under medium-intensity prior land use. The variability with land-use intensity is equivalent to the spread of values in the Zarin *et al.* (2001) data. We emphasize that an understanding of the relationship between biomass accumulation and prior land-use intensity is critical for modeling carbon accumulation in re-growing forests. The CARLUC model probably most closely resembles a medium-intensity land use, because we do not simulate the rapid recovery of biomass produced by sprouting of stumps and roots that occurs following light-intensity land use.

#### *Climate controls on forest productivity*

Across the Amazon, CARLUC predicts a spatial pattern of 20 years aboveground carbon storage that is the same as the pattern for mature forests. Therefore, we agree with Zarin *et al.* (2001) that across the entire Amazon, climate may be an important control on productivity, but suggest that for the sites they present, there is either little enough climate variation so that GSDY is not a significant factor, or that GSDY as defined for the tropics does not capture the impact of climate variation. The spatial pattern of carbon storage in CARLUC clearly reflects the spatial pattern of soil water limitation (Fig. 8).

In areas of adequate soil moisture (i.e.  $f_0$  greater than 0.9), biomass and productivity correlate positively with insolation (Fig. 9). The scatter in Fig. 8 is caused by variability in the  $f_D$  modifier, which describes the limitation on evapotranspiration and carbon fixation due to atmospheric VPD. Insolation is a factor that is not accounted for in the relationship between heat sum index and aboveground biomass presented in Zarin *et al.* (2001). In fact, GSDY and annual insolation appear to be anticorrelated based on our climate and radiation datasets, such that we predict lower biomass levels in the northwest portion of the basin, where the GSDY relationship predicts the highest biomass. Wet areas in

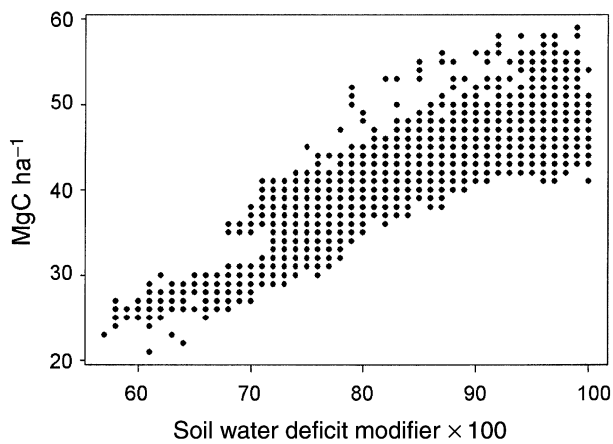


Fig. 8 The relationship between aboveground carbon storage after 20 years of re-growth and the soil water deficit modifier of primary productivity predicted by CARLUC (for CARbon and land-use change).

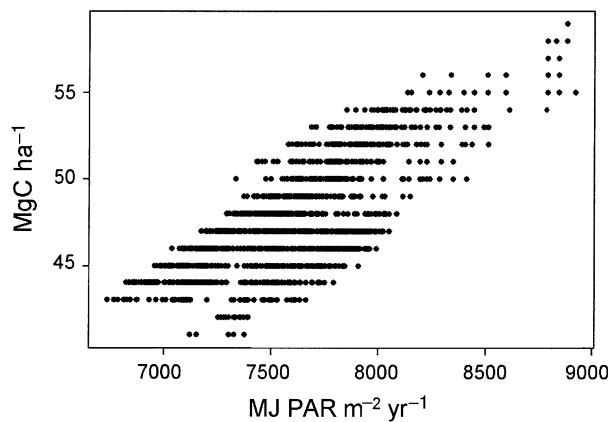


Fig. 9 A graph of total annual photosynthetically active radiation (PAR) flux ( $\text{MJ m}^{-2} \text{yr}^{-1}$ ) vs. aboveground carbon storage after 20 years of re-growth for pixels not experiencing water stress ( $f_g > 0.9$ ).

the Amazon are cloudy for much of the year (Asner, 2001).

Recent basin-wide measurements (Malhi *et al.*, 2003), including areas outside of the Brazilian Legal Amazon, show little relationship between stem growth rate and climatic variables, including average air temperature (a weak relationship which may be more related to a correlation between soil fertility and temperature), annual rainfall, average length of the dry season, and average incoming radiation. It may be the case that the climate forcing of stem growth is masked in this dataset by the differences in soil fertility between volcanically derived upland sites and low-fertility lowland sites. Alternatively, climate variables such as average annual rainfall are only indirectly related to plant available water, which is a function of soil depth and seasonal

changes in the water balance. Since we are only considering the Brazilian Legal Amazon, and not the upland volcanically derived soils, we would expect to see less influence from soil fertility, so that correlations with climate may be more pronounced.

#### Soil carbon dynamics

How representative is the soil model derived from the Trumbore *et al.* (1995) Paragominas study for the entire area impacted by deforestation? Evidence has been gathered that soil carbon storage is lower in sandy vs. nonsandy soils in the Amazon (Silver *et al.*, 2000). We did not address this difference in the model for two reasons. First, sand soils represent a relatively small area in the Legal Amazon, on the order of 7.5% taking the sum of the contributions of Psamments and Podzols from the EMBRAPA soil map (Moraes *et al.*, 1995; Potter *et al.*, 1998). Second, we assume sandy areas are less likely to be cleared for cultivation because of their poor fertility. The Paragominas soil measurements were made in an Oxisol, a deeply weathered clay soil that is very common in eastern and southern Amazonia (Trumbore *et al.*, 1995) where deforestation is concentrated. Further radiocarbon studies should help determine the degree to which the turnover times, humification factor and size of the IOM pool vary in different types of clay soils across the Amazon.

#### Land-cover dynamics

The land-use dynamics in the  $H_{\text{Icluc}}$  experiment cause the ratio of re-growing forest to cumulative deforestation for the Legal Amazon to eventually rise above the 30% value used to set the rate of agricultural abandonment in Houghton *et al.* (2000), almost reaching 50% by 1998. Our simple model suggests that the annual rate of re-clearing of secondary forest rivaled that of primary forest clearing by the late 1990s. The time series of cleared land area is accurately simulated by the  $H_{\text{Icluc}}$  land-cover model (line B in Fig. 10a), while the land-cover change assumed in the  $H_0$  and  $H_{\text{soil}}$  cases leads to an overestimate of cleared area (line A in Fig. 10a) compared with the TRFIC data (line C). The area of secondary forest is overestimated by the  $H_{\text{Icluc}}$  land-cover dynamics (line B in Fig. 10b); however, the area of secondary forest in the TRFIC land-cover maps is likely underestimated, because after about a decade, the spectral signature of secondary forest becomes indistinguishable from primary forest (Alves & Skole, 1996). The degree of underestimation is open to question. The time series of cleared area, and also of secondary forest, predicted by the  $H_0$  and  $H_{\text{Icluc}}$  experiments cross at  $\sim 1983$ , then diverge in the early 1990s. This behavior of

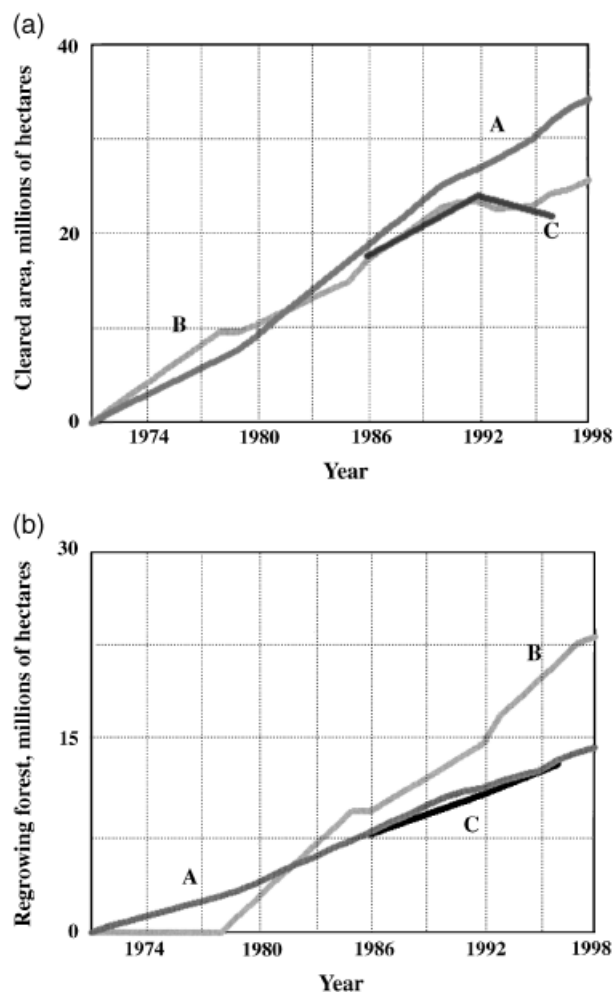


**Fig. 10** (a) Time series of total cleared area in the Brazilian Legal Amazon predicted by the Houghton *et al.* (2000) study (A), predicted by the  $H_{1cluc}$  experiment (B), and calculated from the TRFIC land-cover classification maps from 1986, 1992, and 1996 (c). (b) Time series of secondary forest area in the Brazilian Legal Amazon predicted by the Houghton *et al.* (2000) study (A), predicted by the  $H_{1cluc}$  experiment (B), and calculated from the Tropical Rainforest Information Center (TRFIC) land-cover classification maps from 1986, 1992, and 1996 (c).

land cover causes the crossing of the net flux curves for these two experiments (Fig. 4). The fact that the total amount of carbon released from 1970 to 1998 by land-use change is the same for the  $H_{soil}$  and  $H_{1cluc}$  cases implies that the net flux is driven more by the time series of the deforestation rate than by assumptions of land tenure practices.

The lifetimes of abandoned land and cleared land are consistent with the evolution, over 6 years, of areas identified in Rondônia as being either cleared land (with no secondary vegetation) or secondary forest in 1986, using SPOT imagery (Alves & Skole, 1996). Only

40% of pixels identified as cleared land or secondary forest in 1986 maintained that classification by 1992, underscoring the dynamic nature of land cover in the Amazon, and the degree to which secondary forest is re-cleared for agricultural purposes. By comparison, a pattern of exponential decay with a time constant of 7 years decreases in magnitude by about 40% in 6 years. The results are also consistent with land-use practices in pastures of eastern Amazonia, where roughly 70% of the land is abandoned after 6–12 years of use (Uhl *et al.*, 1988).

In the future, a better way to parameterize the land-use transitions would be to replicate the study of Alves & Skole (1996) of pixel-by-pixel land-cover change for the entire Amazon basin, using the basin-wide land-cover classification maps from TRFIC. However, there are currently problems with the co-registration between images from different years, causing problems for change-detection techniques. One of the most valuable pieces of information for this type of study would be accurate co-registration of the basin-wide TRFIC maps.

#### *The impact of land use on productivity*

We chose not to decrease the primary productivity of secondary forests to reflect the possible impacts of deforestation on soil nutrients. Recent work has indicated that even a long period of shifting cultivation does not adversely impact the concentration of major nutrients in secondary forest tissue (Johnson *et al.*, 2001), so that secondary forest growth may not be more nutrient limited than primary forest. While Amazonian soils are notoriously poor for long-term crop production in the absence of fertilizer addition, forest ecosystems have evolved strategies to efficiently recycle nutrients (Herrera *et al.*, 1978; Stark & Jordan, 1978), and secondary forests may grow quickly enough to recapture nutrients before they are lost through leaching (Harcombe, 1980). There is evidence that the intensity of agriculture, in terms of mechanization and the number of times a pasture is burned, is related to the rate of biomass recovery (Uhl *et al.*, 1988). However, the authors of that study hypothesized that the differences in recovery rate were due to the depletion of tree roots and stumps (which can sprout new aboveground biomass) and the distance of seed sources rather than to changes in nutrient stocks.

#### **Summary and conclusions**

Using CARLUC to simulate forest carbon storage and dynamics but keeping the rest of the model setup the same as the Houghton *et al.* (2000) study (soil and litter carbon dynamics not considered, annual agricultural

abandonment equal to 30% of that year's deforestation) raises the net release of carbon from 1989 to 1998 by 1 PgC. Inclusion of litter and soil carbon dynamics raises the net release of carbon relative to our CARLUC base case ( $H_0$ ) by 1 PgC over the period 1970–1998. Using a different model of land-cover dynamics caused changes in the time series of the annual net flux, but no change in the cumulative release of carbon. Our results suggest that an accurate knowledge of the rate and pattern of deforestation is as important as detailed simulation of ecosystem physiology and carbon cycling for determining the net flux due to deforestation and forest re-growth. In addition, we emphasize that the uncertainty in the net flux due to land-cover change in the Amazon will only be decreased with more precise and geographically distributed measurements of mature forest biomass and carbon dynamics, of the type being collected as part of the LBA-Ecology project. Using a mechanistic model will not achieve this goal on its own, if the model inputs and parameters are uncertain.

In CARLUC, one of the most important and least well-constrained parameters is the turnover time of wood. Wood is the major carbon reservoir in tropical forests on decadal to centennial time scales due to a large carbon input via NPP and a relatively slow turnover time. An understanding of the controls on tropical forest wood turnover time on a regional scale would substantially reduce the uncertainty in this type of study. Currently, as part of LBA and the RAINFOR project (Malhi *et al.*, 2002, 2003), biomass turnover time and stem growth are being measured across the entire Amazon basin, and related to both climatic and edaphic variation. These regional-scale measurements will greatly improve our understanding of the fundamental drivers of carbon dynamics in Neotropical forests, and will be incorporated into future versions of the CARLUC model.

Future work with this model will include study of selective logging and accidental fire impacts on the Amazon carbon budget. A decomposition model that includes sensitivity to seasonal and interannual climate variability could be substituted for the invariant version used here. Lastly, the model will be applied in other regions of the globe to study land-use change and carbon cycle issues.

### Acknowledgements

This research represents a contribution to the large-scale biosphere-atmosphere experiment in Amazonia led by the Brazilian Ministry of Science and Technology. We gratefully acknowledge support from NASA (Terrestrial Ecology Division grant NAG5-9880). The authors would like to thank D. Ray, D.

Nepstad, S. Miller, M. Goulden, A. M. S. Figueira, S. Saleska and Y. Malhi for sharing their research findings, and two anonymous reviewers for their instructive comments.

### References

- Alves DS, Skole DL (1996) Characterizing land cover dynamics using multi-temporal imagery. *International Journal of Remote Sensing*, **17**, 835–839.
- Asner GP (2001) Cloud cover in Landsat observations of the Brazilian Amazon. *International Journal of Remote Sensing*, **22**, 1172–1184.
- Asner GP, Townsend AR, Braswell BH (2000) Satellite observation of El Niño effects on Amazon forest phenology and productivity. *Geophysical Research Letters*, **27**, 981–984.
- Carswell E, Meir P, Wandelli E *et al.* (2000) Photosynthetic capacity in a central Amazonian rain forest. *Tree Physiology*, **20**, 179–186.
- Chambers JQ, Higuchi N, Schimel JP *et al.* (2000) Decomposition and carbon cycling of dead trees in tropical forests of the central Amazon. *Oecologia*, **122**, 380–388.
- Chambers JQ, Higuchi N, Tribuzy ES *et al.* (2001) Carbon sink for a century. *Nature*, **410**, 429–429.
- Chambers JQ, Tribuzy ES, Toledo LC *et al.* (2004) Respiration from a tropical forest ecosystem: partitioning of sources and low carbon use efficiency. *Ecological Applications* (in press).
- Enquist BJ, Niklas KJ (2002) Global allocation rules for patterns of biomass partitioning in seed plants. *Science*, **295**, 1517–1520.
- FAO/UNESCO (1971) *Soil Map of the World. 1:5 000 000*. FAO/UNESCO, Paris.
- Friend AD, Schugart HH, Running SW (1993) A physiology-based gap model of forest dynamics. *Ecology*, **74**, 792–797.
- Gill RA, Jackson RB (2000) Global patterns of root turnover for terrestrial ecosystems. *New Phytologist*, **147**, 13–31.
- Goulden ML, Miller SD, da Rocha HR *et al.* (2003) Physiological controls on tropical forest CO<sub>2</sub> exchange. *Ecological Applications* (in press).
- Granier A, Huc R, Barigah S (1995) Transpiration of natural rain forest and its dependence on climatic factors. *Agricultural and Forest Meteorology*, **78**, 19–29.
- Harcombe PA (1980) Soil nutrient loss as a factor in early tropical secondary succession. *Biotropica*, **12**, 8–15.
- Herrera R, Jordan CF, Klinge H *et al.* (1978) Amazon ecosystems. Their structure and functioning with particular emphasis on nutrients. *Interciencia*, **3**, 223–230.
- Honzak M, Lucas RM, do Amaral I (1996) Estimation of the leaf area index and total biomass of tropical regenerating forests: comparison of methodologies. In: *Amazonian Deforestation and Climate* (eds Gash JHC, Nobre CA, Roberts JM, Victoria RL), pp. 365–381. John Wiley and Sons, New York.
- Houghton RA (2003) Revised estimates of the annual net flux of carbon to the atmosphere from changes in land use and land management 1850–2000. *Tellus*, **55B**, 378–390.
- Houghton RA, Lawrence KT, Hackler JL *et al.* (2001) The spatial distribution of forest biomass in the Brazilian Amazon: a comparison of estimates. *Global Change Biology*, **7**, 731–746.
- Houghton RA, Skole DL, Nobre CA *et al.* (2000) Annual fluxes of carbon from deforestation and regrowth in the Brazilian Amazon. *Nature*, **403**, 301–304.

- Jenkinson DS (1990) The turnover of organic carbon and nitrogen in soil. *Philosophical Transactions of the Royal Society*, **B329**, 361–368.
- Johnson CM, Viera ICG, Zarin DJ *et al.* (2001) Carbon and nutrient storage in primary and secondary forests in eastern Amazonia. *Forest Ecology and Management*, **147**, 245–252.
- Keller M, Palace M, Hurtt G (2001) Biomass estimation in the Tapajos National Forest, Brazil. Examination of sampling and allometric uncertainties. *Forest Ecology and Management*, **154**, 371–382.
- Landsberg JJ, Waring RH (1997) A generalised model of forest productivity using simplified concepts of radiation-use efficiency, carbon balance and partitioning. *Forest Ecology and Management*, **95**, 209–228.
- Malhi Y, Baker TR, Phillips OL *et al.* (2003) The above-ground wood productivity and net primary productivity of 100 neotropical forests. *Global Change Biology* (in press).
- Malhi Y, Phillips OL, Lloyd J *et al.* (2002) An international network to monitor the structure, composition and dynamics of Amazonian forests (RAINFOR). *Journal of Vegetation Science*, **13**, 439–450.
- Manning MR, Melhuish WH (1994) Atmospheric  $\Delta^{14}\text{C}$  record from Wellington. In: *Trends: A Compendium of Data on Global Change*. Carbon Dioxide Information Analysis Center, Oak Ridge National Laboratory, US Department of Energy, Oak Ridge, TN.
- Miller SD, Goulden ML, Menton MC *et al.* (2003) Biometric and micrometeorological measurements of tropical forest carbon balance. *Ecological Applications* (in press).
- Moraes JL, Cerri CC, Melillo JM *et al.* (1995) Soil carbon stocks of the Brazilian Amazon Basin. *Soil Science Society of America Journal*, **59**, 244–247.
- Nascimento HEM, Laurance WF (2002) Total aboveground biomass in central Amazonian rainforests: a landscape-scale study. *Forest Ecology and Management*, **168**, 311–321.
- Nepstad D, Carvalho G, Barros AC *et al.* (2001) Road paving, fire regime feedbacks, and the future of Amazon forests. *Forest Ecology and Management*, **154**, 395–407.
- Nepstad D, de Carvalho CR, Davidson E *et al.* (1994) The role of deep roots in the hydrological and carbon cycles of Amazonian forests and pastures. *Nature*, **372**, 666–669.
- Nepstad DC, Moutinho P, Dias-Filho MB *et al.* (2002) The effects of partial throughfall exclusion on canopy processes, aboveground production and biogeochemistry of an Amazon forest. *Journal of Geophysical Research*, **107**, 8085, doi:10.1029/2001JD000360.
- Nepstad DC, Verissimo A, Alencar A *et al.* (1999) Large-scale impoverishment of Amazonian forests by logging and fire. *Nature*, **398**, 505–508.
- New M, Hulme M, Jones P (1999) Representing twentieth-century space–time climate variability. Part I: development of a 1961–1990 monthly terrestrial climatology. *Journal of Climate*, **12**, 829–856.
- Pinker RT, Laszlo I (1992) Global distribution of photosynthetically active radiation as observed from satellites. *Journal of Applied Meteorology*, **31**, 194–211.
- Potter CS, Davidson EA, Klooster SA *et al.* (1998) Regional application of an ecosystem production model for studies of biogeochemistry in Brazilian Amazonia. *Global Change Biology*, **4**, 315–333.
- Potter C, Genovese VB, Klooster S *et al.* (2001a) Biomass burning losses of carbon estimated from ecosystem modeling and satellite data analysis for the Brazilian Amazon region. *Atmospheric Environment*, **35**, 1773–1781.
- Potter C, Klooster S, de Carvalho CR *et al.* (2001b) Modeling seasonal and interannual variability in ecosystem carbon cycling for the Brazilian Amazon region. *Journal of Geophysical Research*, **106**, 10423–10446.
- Prentice IC, Farquhar GD, Fasham MJR *et al.* (2001) In: *Climate Change 2001: The Scientific Basis. Contribution of Working Group I to the Third Assessment Report of the Intergovernmental Panel on Climate Change* (ed. Johnson CA), pp. 183–237. Cambridge University Press, Cambridge, UK.
- Prince SD, Goward SN (1995) Global primary production: a remote sensing approach. *Journal of Biogeography*, **22**, 815–835.
- Rice AH, Pyle EH, Saleska SR *et al.* (2003) Carbon balance and vegetation dynamics of an old-growth tropical forest. *Ecological Applications*, in press.
- Roberts JM, Cabral OMR, da Costa JP *et al.* (1996) An overview of the leaf area index and physiological measurements during ABRACOS. In: *Amazonian Deforestation and Climate* (ed. Victoria RL), pp. 287–305. John Wiley and Sons, New York.
- Saldarriaga JG, Luxmoore RJ (1991) Solar energy conversion efficiencies during succession of a tropical rain forest in Amazonia. *Journal of Tropical Ecology*, **7**, 233–242.
- Salimon CI, Brown IF (2000) Secondary forests in western Amazonia: significant sinks for carbon released by deforestation? *Interciencia*, **25**, 198–202.
- Silver WL, Neff J, McGroddy M *et al.* (2000) Effects of soil texture on belowground carbon and nutrient storage in a lowland Amazonian forest ecosystem. *Ecosystems*, **3**, 193–209.
- Skole D, Tucker C (1993) Tropical deforestation and habitat fragmentation in the Amazon: satellite data from 1978 to 1988. *Science*, **260**, 1905–1910.
- Soil Survey Staff (1990) Keys to soil taxonomy, fourth edition. *SMSS technical monograph no. 6*. Blacksburg, Virginia.
- Stark NM, Jordan CF (1978) Nutrient retention by the root mat of an Amazonian rain forest. *Ecology*, **59**, 434–437.
- Stone TA, Schlesinger P, Woodwell GM *et al.* (1994) A map of the vegetation of South America based on satellite imagery. *Photogrammetric Engineering and Remote Sensing*, **60**, 541–551.
- Stuiver M, Reimer PJ, Bard E *et al.* (1998) Intcal98 radiocarbon age calibration, 24 000–0 cal BP. *Radiocarbon*, **40**, 1041–1083.
- Thompson MV, Randerson JT (1999) Impulse response functions of terrestrial carbon models: method and application. *Global Change Biology*, **5**, 371–394.
- Tian HQ, Melillo JM, Kicklighter DW *et al.* (1998) Effect of interannual climate variability on carbon storage in Amazonian ecosystems. *Nature*, **396**, 664–667.
- Trumbore SE, Davidson EA, de Camargo PB *et al.* (1995) Belowground cycling of carbon in forests and pastures of Eastern Amazonia. *Global Biogeochemical Cycles*, **9**, 515–528.
- Uhl C, Buschbacher R, Serrao EAS (1988) Abandoned pastures in Eastern Amazonia. I. Patterns of plant succession. *Journal of Ecology*, **76**, 663–681.
- Zarin DJ, Ducey MJ, Tucker JM (2001) Potential biomass accumulation in Amazonian regrowth forests. *Ecosystems*, **4**, 658–668.